A&A 494, 719–727 (2009)
DOI: 10.1051/0004-6361:200810570

Astronomy & Astrophysics

On the frequency of N_2H^+ and N_2D^+⋆ *(Research Note)*

L. Pagani[1], F. Daniel[1,2], and M.-L. Dubernet[1]

[1] LERMA & UMR8112 du CNRS, Observatoire de Paris, 61 Av. de l'Observatoire, 75014 Paris, France
e-mail: [laurent.pagani;marie-lise.dubernet]@obspm.fr
[2] Department of Molecular and Infrared Astrophysics (DAMIR), Consejo Superior de Investigaciones Científicas (CSIC), C/ Serrano 121, 28006 Madrid, Spain
e-mail: daniel@damir.iem.csic.es

Received 11 July 2008 / Accepted 10 November 2008

ABSTRACT

Context. Dynamical studies of prestellar cores search for small velocity differences between different tracers. The highest radiation frequency precision is therefore required for each of these species.
Aims. We want to adjust the frequency of the first three rotational transitions of N_2H^+ and N_2D^+ and extrapolate to the next three transitions.
Methods. We compare N_2H^+ and N_2D^+ to NH_3, the frequency of which is more accurately known and which has the advantage of being spatially coexistent with N_2H^+ and N_2D^+ in dark cloud cores. With lines among the narrowest, and the N_2H^+ and NH_3 emitting region among the largest, L183 is a good candidate for comparing these species.
Results. A correction of ∼10 kHz for the N_2H^+ (J: 1−0) transition is found (∼0.03 km s^{-1}). Similar corrections from a few m s^{-1} up to ∼0.05 km s^{-1} compared to previous astronomical determinations are reported for the other transitions (N_2H^+ (J: 3−2) and N_2D^+(J: 1−0), (J: 2−1), and (J: 3−2)). Einstein spontaneous-decay coefficients (A_{ul}) are included.

Key words. molecular data – ISM: kinematics and dynamics – radio lines: ISM

1. Introduction

In the quest for star-forming cores, kinematic studies play a crucial role by trying to unveil either the slowly contracting cores or the fast collapsing ones, depending upon which theory we rely upon or at what moment along the evolutionary track the prestellar core is standing. As already discussed by Lee et al. (1999), accurate knowledge of every species' line frequency is of utmost importance in tracking small systematic velocity gradients in molecular clouds. Because these velocity shifts can be as small as a few tens of m s^{-1}, millimeter line transitions should be known with a precision of at least 10^{-7} and ideally 10^{-8}. Some species are easily measured in the laboratory, especially stable species like CO, NH_3, etc. Others are unstable and more difficult to measure (such as OH, H_2D^+, etc.). One possibility in the latter case is to compare the transitions of those species with the transitions of another well-known species in dark cloud cores where the lines are narrow enough to be accurately measured. However, the obvious difficulty is to be sure that the two species share the same volume in the cloud and undergo the same macroscopic velocity shifts. Even so, the line opacities might be a problem if too different in presence of a velocity gradient causing the two coexistent species to then emphasize different parts of the cloud, depending on the depth at which their respective opacity reaches 1. A problem of opacity was indeed met in the comparison of CS with CCS made by Kuiper et al. (1996) in their attempt to measure the frequency of the CS lines, as discussed in Pagani et al. (2001).

Caselli et al. (1995) performed such a measurement for N_2H^+, comparing N_2H^+ (J: 1−0) line emission to the C_3H_2 ($J_{KK'}$: 2_{12}−1_{01}) line emission in L1512, confirming a sizeable difference between laboratory measurements and astronomical observations. Expanding on a previous work by Gerin et al. (2001), Dore et al. (2004) also calculated and observed the N_2D^+ (J: 1−0) transition in L183, and extrapolated to the higher N_2D^+ transitions (giving slightly different values compared to Gerin et al. 2001, for the J: 2−1 and J: 3−2 transitions). They aligned their N_2D^+ (J: 1−0) observation onto their N_2H^+ (J: 1−0) towards the same source with the same telescope. The N_2H^+ rotational constant was itself redetermined from a new evaluation of the N_2H^+ (J: 1−0) frequency, itself from a comparison with $C^{18}O$ (J: 1−0) in the L1512 cloud (see Dore et al. 2004, for more details). This new value gave an offset of −4.2 kHz from their previous determination.

While the direct comparison of the N_2D^+ and N_2H^+ lines is presently the best option because N_2H^+ must exist where N_2D^+ exists, the hypothesis that C_3H_2 is also present in the same volume as N_2H^+ is more questionable because of differential depletion problems. Dore et al. (2004) also note that using $C^{18}O$ has the problem of tracing different regions but, hoped for a null velocity shift between the two tracers. We think that a better

⋆ Based on observations made with the IRAM 30-m and the GBT 100-m. IRAM is supported by INSU/CNRS (France), MPG (Germany), and IGN (Spain). GBT is run by the National Radio Astronomy Observatory, which is a facility of the National Science Foundation operated under cooperative agreement by Associated Universities, Inc.

possibility exists for accurately measuring the frequency of N_2H^+, namely by taking NH_3 as the frequency reference. It is clear that NH_3 and N_2H^+ are coexistent species in depleted prestellar cores (e.g. Tafalla et al. 2002, 2004), because they have a common chemical origin and show similar extents in most cores.

In this Note, we present a detailed comparison of NH_3 with N_2H^+ and N_2D^+ in L183, checking that the measurable velocity shifts across the core are the same for all three species, to convince ourselves of their coexistence and the absence of any opacity effect on the velocity peak position. Schmid-Burgk et al. (2004) have developed a similar strategy in their study of the $H^{13}CO^+$ and ^{13}CO hyperfine structure (hereafter HFS) towards another dark cloud, L1512, with similar very narrow linewidths. With these comparisons in hand, we give all corrections for the 5 most currently observed transitions, together with their Einstein spontaneous decay coefficients (A_{ul}), determine the best-fitting rotational constants and compute the expected frequencies for the next 3 rotational transitions (J: 4–3, 5–4, 6–5).

2. Observations

The whole elongated dense core of L183 (reference position: $\alpha_{2000} = 15^h54^m08.5^s$ $\delta_{2000} = -2°52'48''$) has now been fully mapped wih the IRAM 30-m telescope in a series of observations spanning several years from November 2003 to July 2007. The N_2H^+ and N_2D^+ (J: 1–0) lines were fully mapped, while the N_2H^+ (J: 3–2), N_2D^+ (J: 2–1) and (J: 3–2) lines were mapped mostly towards the main core and its elongated ridge and partly towards the peak of the northern core (see Pagani et al. 2004, 2005). All observations were performed in frequency-switch mode. For the (J: 1–0) lines, the frequency sampling is 10 kHz, 10, or 20 kHz for the (J: 2–1) and 40 kHz for the (J: 3–2) lines, providing comparable velocity resolution for all lines in the range 30–50 m s^{-1}. Spatial resolution ranges from 33″ at 77 GHz to 9″ at 279 GHz. For all lines, the spatial sampling is 12″ for the main prestellar core and 15″ for the southern extension and for the northern prestellar core. We used Caselli et al. (1995) and Dore et al. (2004) frequencies for N_2H^+ and N_2D^+ transitions, respectively.

We observed NH_3 (1, 1) and (2, 2) inversion lines towards the whole core at the new Green Bank 100-m telescope (GBT) in November 2006 and March 2007, with velocity sampling of 20 m s^{-1} and a typical T_{sys} of 50 K, in frequency-switch mode. The angular resolution (~35″) is close to that of the 30-m for the low-frequency (J: 1–0) N_2D^+ line. The spatial sampling is 24″ all over the source. We used the accurate measurement of Kukolich (1967) for NH_3 (1, 1), namely ν = 23 694 495 487 (±48) Hz, which is an average estimated from the whole HFS (see also Hougen 1972, who revisited the NH_3 and $^{15}NH_3$ frequencies. The reported accuracy is higher but the NH_3 (1, 1) frequency remains basically unchanged, namely ν = 23 694 495 481 ± 22 Hz). For this frequency, the two strongest hyperfine components have the following frequency offsets:

$$\Delta\nu(F_1F\colon 2,^5/_2 \rightarrow 2,^5/_2) = 10\,463 \text{ Hz}$$

$$\Delta\nu(F_1F\colon 2,^3/_2 \rightarrow 2,^3/_2) = -15\,196 \text{ Hz}.$$

Samples of these spectra (N_2H^+, N_2D^+ and NH_3) are displayed in Pagani et al. (2007).

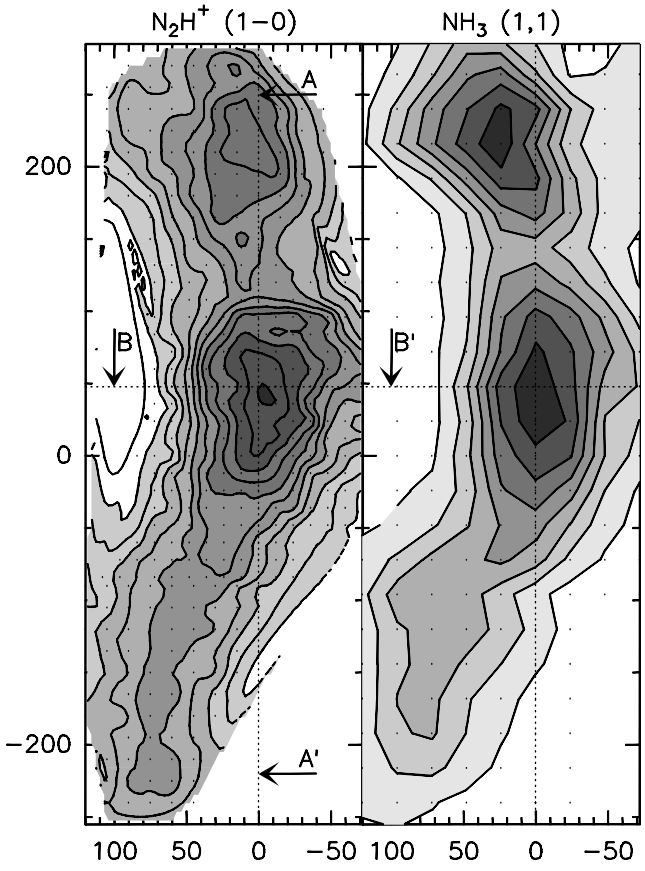

Fig. 1. N_2H^+ (J: 1–0) (*left*) and NH_3 (1, 1) (*right*) integrated intensity maps. The dotted lines AA′ and BB′ indicate the profiles along which the velocity gradients are traced in Figs. 2 and 3. Reference position: $\alpha_{2000} = 15^h54^m08.5^s$ $\delta_{2000} = -2°52'48''$.

3. Spatial coexistence of ammonia and diazenylium

Though depletion of molecules was predicted in the 70s, it was only a few years after the publication of the Caselli et al. (1995) paper on the frequency of N_2H^+ that depletion was actually discovered and traced (e.g. Willacy et al. 1998). Therefore the hypothesis made by Caselli et al. (1995) that C_3H_2 and N_2H^+ are spatially coexistent is probably refutable, because it is clear now that such a heavy carbon carrier should be depleted in the same region as CO, which is the region where N_2H^+ appears. Indeed, the detection of N_2D^+ in L1512 as a large fraction of N_2H^+ (Roberts & Millar 2007) is a clear sign of heavy depletion of other molecules. Therefore the velocity coincidence between these two species is questionable.

Ammonia and diazenylium have the same chemical origin, starting from N_2 and are well-known to be coexistent, as discussed by e.g. Tafalla et al. (2002, 2004). This is particularly true in L183 as can be seen in Fig. 1 (but not for C_3H_2 which is much less extented, mostly concentrated towards the northern prestellar core, as can be seen in Swade 1989). Interestingly, the velocity along the dense filament is constantly changing (Fig. 2), evoking a flow towards the prestellar cores, and the cut perpendicular to the filament (marked BB′ in Fig. 1) suggests a rotation of the filament around its vertical axis (Fig. 3). The NH_3 (1, 1), N_2H^+ and N_2D^+ (J: 1–0) lines all trace exactly the same gradients so it seems compulsory that the velocities of the different compounds be identical, as there is no obvious possibility that

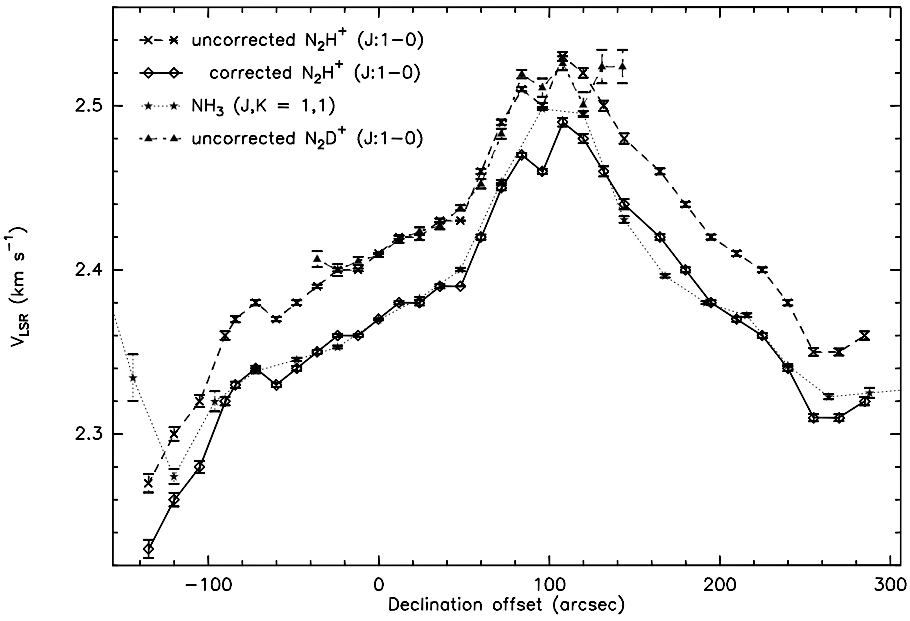

Fig. 2. N_2H^+, N_2D^+ (J: 1−0) and NH_3 (1, 1) line of sight velocity along the AA′ cut (see Fig. 1). The N_2H^+ data are displayed with the original frequency (uncorrected) and with a correction of −41 m s^{-1}. The uncorrected N_2D^+ (J: 1−0) points are consistent with the uncorrected N_2H^+ points despite the different opacities.

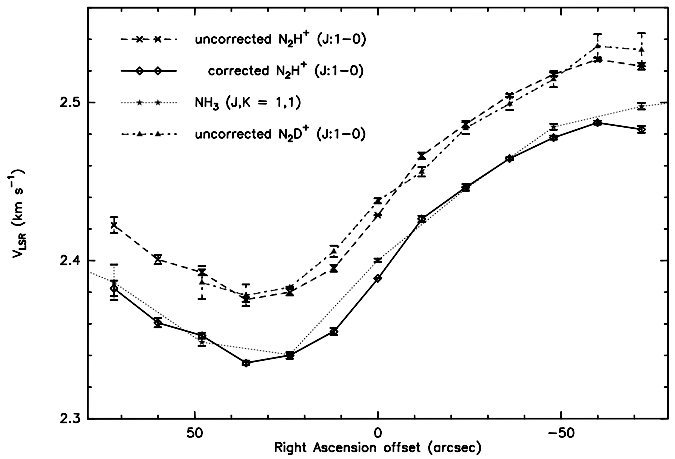

Fig. 3. N_2H^+, N_2D^+ (J: 1−0) , and NH_3 (1, 1) line-of-sight velocity along the BB′ cut (see Fig. 1). The N_2H^+ data are displayed with the original frequency (uncorrected) and with a correction of −41 m s^{-1}. The uncorrected N_2D^+ (J: 1−0) points are consistent with the uncorrected N_2H^+ points despite the different opacities.

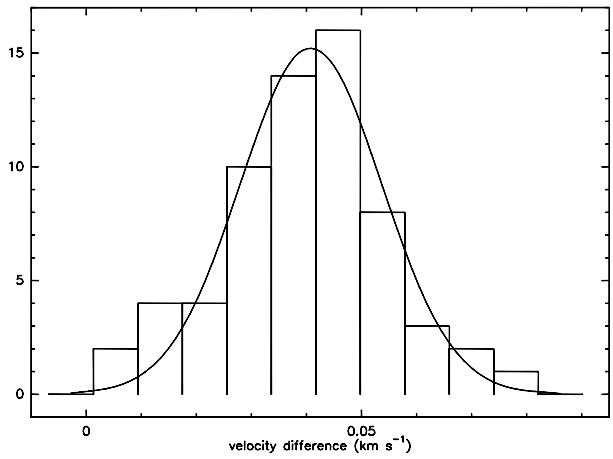

Fig. 4. N_2H^+ (J: 1−0) and NH_3 (1, 1) line-of-sight velocity difference histogram. The Gaussian fit is centered on 40.8 m s^{-1} with a dispersion σ = 12.9 m s^{-1}.

the velocity gradients be exactly parallel and offset from each other, especially in the probable case of the cylinder rotation. With the present N_2H^+ (J: 1−0) frequency as given by Caselli et al. (1995), there is indeed a clear offset with respect to the NH_3 velocity gradient, close to 40 m s^{-1} (and to 26 m s^{-1} compared to the new value in Dore et al. 2004). Amano et al. (2005) also have reinterpreted Caselli et al. (1995) observations along with new laboratory measurements but are therefore plagued by the velocity difference between N_2H^+ and C_3H_2, which appears to exist in view of the present discrepancy between NH_3 and N_2H^+. Consequently, their best fit (#2 of their Table 2) is to be considered with caution. Finally, that N_2D^+ velocity centroids are almost identical to those of N_2H^+ indicates that the different opacities of the lines do not introduce any measurable bias here (though a very tiny shift is possibly visible in Fig. 3 where the N_2D^+ displacement is symmetrically slightly less than the N_2H^+ displacement).

Table 1. Rotation (B) and centrifugal distortion (D) constants for N_2H^+ and N_2D^+, with errors in parentheses given for the last two digits.

Species	B MHz	D MHz
N_2H^+	46586.8713(25)	0.08796(24)
N_2D^+	38554.7479(17)	0.06181(15)

In conclusion, the three species are spatially coexistent and trace the same velocities, and one must adjust the frequencies of N_2H^+ and N_2D^+ to that of NH_3.

4. Frequency corrections

4.1. N_2H^+ (J: 1–0) correction

Frequency was measured using the MINIMIZE function in CLASS[1] with the HFS method for all species. For NH_3, the

[1] http://www.iram.fr/IRAMFR/GILDAS

Table 2. Hyperfine components and A_{ul} Einstein spontaneous emission coefficients of the (J: 1−0) transition of N_2H^+.

J'	F'_1	$F' \rightarrow J$		F_1	F	Frequency[a] (MHz)	A_{ul} (s^{-1})
1	1	0	0	1	1	93 171.6081	3.628(−5)[b]
1	1	2	0	1	2	93 171.9049	2.721(−5)
1	1	2	0	1	1	93 171.9049	9.069(−6)
1	1	1	0	1	0	93 172.0398	1.209(−5)
1	1	1	0	1	2	93 172.0398	1.512(−5)
1	1	1	0	1	1	93 172.0398	9.069(−6)
1	2	2	0	1	1	93 173.4669	2.721(−5)
1	2	2	0	1	2	93 173.4669	9.070(−6)
1	2	3	0	1	2	93 173.7637	3.628(−5)
1	2	1	0	1	2	93 173.9540	1.008(−6)
1	2	1	0	1	1	93 173.9540	1.512(−5)
1	2	1	0	1	0	93 173.9540	2.016(−5)
1	0	1	0	1	1	93 176.2522	1.209(−5)
1	0	1	0	1	2	93 176.2522	2.016(−5)
1	0	1	0	1	0	93 176.2522	4.031(−6)

[a] The frequency uncertainty is ±4.0 kHz for all hyperfine components; [b] 3.628(−5) means 3.628×10^{-5}.

Table 3. Hyperfine components and A_{ul} Einstein spontaneous emission coefficients of the (J: 2−1) transition of N_2H^+.

J'	F'_1	$F' \rightarrow J$		F_1	F	Frequency[a] (MHz)	A_{ul} (s^{-1})
2	2	2	1	2	1	186 342.4666	1.306(−5)
2	2	2	1	2	3	186 342.6570	1.354(−5)
2	2	1	1	2	1	186 342.7883	6.530(−5)
2	2	3	1	2	3	186 342.9123	7.739(−5)
2	2	2	1	2	2	186 342.9537	6.046(−5)
2	1	1	1	0	1	186 343.0459	1.935(−4)
2	2	3	1	2	2	186 343.2091	9.674(−6)
2	1	2	1	0	1	186 343.2577	1.935(−4)
2	2	1	1	2	2	186 343.2755	2.177(−5)
2	1	0	1	0	1	186 343.5098	1.935(−4)
2	2	2	1	1	1	186 344.3808	1.959(−4)
2	3	3	1	2	3	186 344.4444	3.870(−5)
2	2	2	1	1	2	186 344.5158	6.530(−5)
2	2	1	1	1	1	186 344.7026	1.088(−4)
2	3	3	1	2	2	186 344.7412	3.096(−4)
2	3	2	1	2	1	186 344.7615	2.925(−4)
2	2	3	1	1	2	186 344.7711	2.612(−4)
2	2	1	1	1	2	186 344.8375	7.255(−6)
2	3	4	1	2	3	186 344.8419	3.483(−4)
2	3	2	1	2	3	186 344.9519	1.548(−6)
2	2	1	1	1	0	186 345.1343	1.451(−4)
2	3	2	1	2	2	186 345.2487	5.417(−5)
2	1	1	1	2	1	186 345.3441	2.418(−6)
2	1	2	1	2	1	186 345.5559	9.674(−8)
2	1	2	1	2	3	186 345.7462	8.126(−6)
2	1	0	1	2	1	186 345.8080	9.674(−6)
2	1	1	1	2	2	186 345.8312	7.256(−6)
2	1	2	1	2	2	186 346.0430	1.451(−6)
2	1	1	1	1	1	186 347.2584	3.628(−5)
2	1	1	1	1	2	186 347.3933	6.046(−5)
2	1	2	1	1	1	186 347.4701	3.628(−5)
2	1	2	1	1	2	186 347.6050	1.088(−4)
2	1	1	1	1	0	186 347.6901	4.837(−5)
2	1	0	1	1	1	186 347.7222	1.451(−4)

[a] The frequency uncertainty is ±2.3 kHz for all hyperfine components.

HFS method is similar to the internally built NH3(1, 1) method. Because it is easier to deal with velocity offsets in CLASS,

Table 4. Hyperfine components and A_{ul} Einstein spontaneous emission coefficients of the (J: 3−2) transition of N_2H^+.

J'	F'_1	$F' \rightarrow J$		F_1	F	Frequency[a] (MHz)	A_{ul} (s^{-1})
3	3	3	2	3	2	279 509.361	1.110(−5)
3	3	3	2	3	4	279 509.471	1.124(−5)
3	3	2	2	3	2	279 509.795	1.244(−4)
3	3	4	2	3	4	279 509.849	1.312(−4)
3	3	3	2	3	3	279 509.868	1.176(−4)
3	3	4	2	3	3	279 510.246	8.745(−6)
3	3	2	2	3	3	279 510.302	1.555(−5)
3	2	2	2	1	2	279 511.103	2.644(−4)
3	2	2	2	1	1	279 511.315	7.933(−4)
3	2	1	2	1	0	279 511.355	5.876(−4)
3	4	4	2	3	4	279 511.384	7.870(−5)
3	3	3	2	2	3	279 511.401	1.244(−4)
3	2	3	2	1	2	279 511.479	1.058(−3)
3	2	1	2	1	2	279 511.607	2.938(−5)
3	3	3	2	2	2	279 511.656	9.950(−4)
3	3	2	2	2	1	279 511.768	9.402(−4)
3	3	4	2	2	3	279 511.778	1.119(−3)
3	4	3	2	3	2	279 511.780	1.156(−3)
3	4	4	2	3	3	279 511.781	1.181(−3)
3	2	1	2	1	1	279 511.819	4.407(−4)
3	4	5	2	3	4	279 511.832	1.259(−3)
3	3	2	2	2	3	279 511.834	4.975(−6)
3	4	3	2	3	4	279 511.890	1.606(−6)
3	2	2	2	3	2	279 511.897	6.218(−7)
3	3	2	2	2	2	279 512.090	1.741(−4)
3	2	3	2	3	2	279 512.273	1.269(−8)
3	4	3	2	3	3	279 512.287	1.012(−4)
3	2	3	2	3	4	279 512.383	5.140(−6)
3	2	1	2	3	2	279 512.401	5.597(−6)
3	2	2	2	3	3	279 512.405	4.975(−6)
3	2	3	2	3	3	279 512.781	4.442(−7)
3	2	2	2	2	1	279 513.870	2.938(−5)
3	2	2	2	2	3	279 513.937	3.047(−5)
3	2	2	2	2	2	279 514.192	1.360(−4)
3	2	3	2	2	3	279 514.313	1.741(−4)
3	2	1	2	2	1	279 514.374	1.469(−4)
3	2	3	2	2	2	279 514.568	2.177(−5)
3	2	1	2	2	2	279 514.696	4.897(−5)

[a] The frequency uncertainty is ±11 kHz for all hyperfine components.

especially as we have to compare two species at different frequencies, the measurements have all been made on the velocity scale. Velocity differences are subsequently converted into frequency offsets using the approximate Doppler-shift formula ($\nu = \nu_0(1 - \frac{\delta v}{c})$, δv being the velocity offset, c the celerity of light, ν and ν_0 the corrected and original frequencies). To fit all the hyperfine components individually, the HFS method requires that we provide their list with their relative velocities and relative weights, these parameters not being adjusted during the fit. Therefore, we used the detailed HFS provided by Caselli et al. (1995), Dore et al. (2004), and Kukolich (1967). Since an accurate determination of the hyperfine spectroscopic constants only slightly depends on the adopted rotational constants B and D[2], we can safely use the previously determined ones. In doing so, our own determination for the relative velocity offsets between the hyperfine components in the J: 1−0 line agree with

[2] Indeed, it can be noted that the HFS splitting is, in a first approximation, identical for both N_2H^+ and N_2D^+despite a large, ~20% variation in B rotational constant

Table 5. Hyperfine components and A_{ul} Einstein spontaneous emission coefficients of the (J: 4–3) transition of N_2H^+.

J'	F_1'	$F' \rightarrow J$		F_1	F	Frequency[a] (MHz)	A_{ul} (s^{-1})
4	4	4	3	4	3	372 670.005	9.404(−6)
4	4	4	3	4	5	372 670.062	9.457(−6)
4	4	3	3	4	3	372 670.467	1.814(−4)
4	4	5	3	4	5	372 670.500	1.857(−4)
4	4	4	3	4	4	372 670.510	1.746(−4)
4	4	5	3	4	4	372 670.948	7.738(−6)
4	4	3	3	4	4	372 670.972	1.209(−5)
4	3	3	3	2	3	372 671.904	3.158(−4)
4	5	5	3	4	5	372 672.046	1.238(−4)
4	4	4	3	3	4	372 672.046	1.814(−4)
4	3	3	3	2	2	372 672.280	2.527(−3)
4	3	2	3	2	1	372 672.280	2.388(−3)
4	3	4	3	2	3	372 672.348	2.843(−3)
4	3	3	3	4	3	372 672.398	2.467(−7)
4	3	2	3	2	3	372 672.408	1.263(−5)
4	4	4	3	3	3	372 672.423	2.720(−3)
4	4	3	3	3	2	372 672.452	2.665(−3)
4	4	5	3	3	4	372 672.484	2.902(−3)
4	5	4	3	4	3	372 672.486	2.942(−3)
4	5	5	3	4	4	372 672.494	2.971(−3)
4	4	3	3	3	4	372 672.508	3.701(−6)
4	5	6	3	4	5	372 672.526	3.095(−3)
4	5	4	3	4	5	372 672.544	1.528(−6)
4	3	2	3	2	2	372 672.784	4.422(−4)
4	3	4	3	4	3	372 672.842	3.046(−9)
4	4	3	3	3	3	372 672.885	2.332(−4)
4	3	4	3	4	5	372 672.899	3.753(−6)
4	3	2	3	4	3	372 672.902	3.948(−6)
4	3	3	3	4	4	372 672.903	3.701(−6)
4	5	4	3	4	4	372 672.992	1.513(−4)
4	3	4	3	4	4	372 673.347	1.919(−7)
4	3	3	3	3	2	372 674.383	1.974(−5)
4	3	3	3	3	4	372 674.439	1.999(−5)
4	3	3	3	3	3	372 674.816	2.090(−4)
4	3	4	3	3	4	372 674.883	2.332(−4)
4	3	2	3	3	2	372 674.887	2.211(−4)
4	3	4	3	3	3	372 675.260	1.555(−5)
4	3	2	3	3	3	372 675.320	2.764(−5)

[a] The frequency uncertainty is ±41 kHz for all hyperfine components.

Table 6. Hyperfine components and A_{ul} Einstein spontaneous emission coefficients of the (J: 5–4) transition of N_2H^+.

J'	F_1'	$F' \rightarrow J$		F_1	F	Frequency[a] (MHz)	A_{ul} (s^{-1})
5	5	5	4	5	4	465 822.236	8.093(−6)
5	5	5	4	5	6	465 822.254	8.118(−6)
5	5	4	4	5	4	465 822.704	2.374(−4)
5	5	6	4	5	6	465 822.729	2.404(−4)
5	5	5	4	5	5	465 822.734	2.311(−4)
5	5	4	4	5	5	465 823.202	9.891(−6)
5	5	6	4	5	5	465 823.209	6.869(−6)
5	4	4	4	3	4	465 824.191	3.673(−4)
5	5	5	4	4	5	465 824.279	2.374(−4)
5	6	6	4	5	6	465 824.285	1.717(−4)
5	4	4	4	5	4	465 824.546	1.221(−7)
5	4	3	4	3	2	465 824.627	5.397(−3)
5	4	4	4	3	3	465 824.635	5.509(−3)
5	4	5	4	3	4	465 824.673	5.877(−3)
5	4	3	4	3	4	465 824.687	7.496(−6)
5	5	5	4	4	4	465 824.717	5.697(−3)
5	5	4	4	4	3	465 824.723	5.642(−3)
5	5	4	4	4	5	465 824.747	2.931(−6)
5	5	6	4	4	5	465 824.754	5.935(−3)
5	6	5	4	5	4	465 824.756	5.978(−3)
5	6	6	4	5	5	465 824.765	6.010(−3)
5	6	5	4	5	6	465 824.774	1.419(−6)
5	6	7	4	5	6	465 824.788	6.182(−3)
5	4	5	4	5	4	465 825.029	1.009(−9)
5	4	3	4	5	4	465 825.042	3.053(−6)
5	4	4	4	5	5	465 825.045	2.931(−6)
5	4	5	4	5	6	465 825.047	2.952(−6)
5	4	3	4	3	3	465 825.131	4.722(−4)
5	5	4	4	4	4	465 825.185	2.901(−4)
5	6	5	4	5	5	465 825.254	2.029(−4)
5	4	5	4	5	5	465 825.527	9.991(−8)
5	4	4	4	4	3	465 826.566	1.469(−5)
5	4	4	4	4	5	465 826.590	1.478(−5)
5	4	4	4	4	4	465 827.028	2.728(−4)
5	4	3	4	4	3	465 827.062	2.833(−4)
5	4	5	4	4	5	465 827.072	2.902(−4)
5	4	5	4	4	4	465 827.510	1.209(−5)
5	4	3	4	4	4	465 827.524	1.889(−5)

[a] The frequency uncertainty is ±95 kHz for all hyperfine components.

Caselli et al. (1995) with a typical dispersion of 0.7 kHz. Though this is twice as much as the rms error on our frequency determination of each individual component ($\sigma \sim 0.3$ kHz), we find that using their offsets or ours introduces a negligible difference of 0.13 kHz in the J: 1–0 transition frequency determination, which is comparable to the rms error of the fit (0.12 kHz). We also did not find any improvement on the rms error of the fit itself. For the N_2H^+ and N_2D^+ transitions, the strongest hyperfine transition was given null velocity offset, as it was also the strongest hyperfine transition frequency used to tune the receivers. The advantage of a complex and strong HFS is that it lowers the uncertainty on the velocity fit, compared to a single line estimate (fitting the N_2H^+ J: 1–0 lines individually with independent Gaussians, gives errors between 0.85 and 1.2 m s^{-1} instead of 0.38 m s^{-1} with the global HFS fit for the reference spectrum).

Though the reference position has been observed often enough to get very high signal-to-noise ratios for most transitions, it seems more secure to measure the offset between N_2H^+ and NH_3 on all common positions (every other position in the central core, a few positions in the rest of the cloud) and measure the average difference. We have identified 65 common positions with sufficient signal-to-noise ratios and obtained the dispersion histogram of the velocity difference (Fig. 4). After fitting the histogram with a Gaussian, we find a velocity difference of 40.8 m s^{-1} with a dispersion $\sigma = 12.9$ m s^{-1}. This corresponds to a frequency correction of −13 ± 4 kHz (or −8.8 kHz compared to Dore et al. 2004). For the reference position alone, the difference is also 40.8 m s^{-1} with an error $\sigma = 0.56$ m s^{-1} (due to the very high signal-to-noise ratio obtained for both lines towards that position).

4.2. N_2H^+ (J: 3–2) correction

For the N_2H^+ (J: 3–2) transition, only the reference position has been observed with a reasonably good signal-to-noise ratio (~10). Therefore, we can only make a direct comparison for this position. The Jet Propulsion Laboratory (JPL) catalog frequency for this line (279 511.701 ± 0.05 MHz) is too vague to be useful for a precise velocity determination. The Cologne

Table 7. Hyperfine components and A_{ul} Einstein spontaneous emission coefficients of the (J: 6−5) transition of N_2H^+.

J'	F_1'	$F' \rightarrow J$		F_1	F	Frequency[a] (MHz)	A_{ul} (s^{-1})
6	6	6	5	6	7	558 963.91	7.094(−6)
6	6	6	5	6	5	558 963.93	7.081(−6)
6	6	5	5	6	5	558 964.39	2.929(−4)
6	6	7	5	6	7	558 964.41	2.951(−4)
6	6	6	5	6	6	558 964.42	2.871(−4)
6	6	5	5	6	6	558 964.88	8.368(−6)
6	6	7	5	6	6	558 964.92	6.148(−6)
6	5	5	5	4	5	558 965.91	4.195(−4)
6	6	6	5	5	6	558 965.97	2.929(−4)
6	7	7	5	6	7	558 965.98	2.213(−4)
6	5	5	5	6	5	558 966.18	6.916(−8)
6	5	4	5	4	3	558 966.38	9.969(−3)
6	5	5	5	4	4	558 966.39	1.007(−2)
6	5	4	5	4	5	558 966.39	5.179(−6)
6	5	6	5	4	5	558 966.42	1.049(−2)
6	6	5	5	5	6	558 966.44	2.421(−6)
6	6	5	5	5	4	558 966.44	1.020(−2)
6	6	6	5	5	5	558 966.45	1.025(−2)
6	7	6	5	6	7	558 966.46	1.310(−6)
6	6	7	5	5	6	558 966.47	1.054(−2)
6	7	6	5	6	5	558 966.47	1.059(−2)
6	7	7	5	6	6	558 966.48	1.062(−2)
6	7	8	5	6	7	558 966.50	1.085(−2)
6	5	4	5	6	5	558 966.67	2.490(−6)
6	5	5	5	6	6	558 966.67	2.421(−6)
6	5	6	5	6	7	558 966.68	2.431(−6)
6	5	6	5	6	5	558 966.69	4.092e−10
6	5	4	5	4	4	558 966.88	5.127(−4)
6	6	5	5	5	5	558 966.91	3.462(−4)
6	7	6	5	6	6	558 966.96	2.554(−4)
6	5	6	5	6	6	558 967.18	5.852(−8)
6	5	5	5	5	6	558 968.27	1.169(−5)
6	5	5	5	5	4	558 968.23	1.165(−5)
6	5	5	5	5	5	558 968.70	3.327(−4)
6	5	4	5	5	4	558 968.72	3.418(−4)
6	5	6	5	5	6	558 968.74	3.462(−4)
6	5	4	5	5	5	558 969.19	1.424(−5)
6	5	6	5	5	5	558 969.21	9.890(−6)

[a] The frequency uncertainty is ±0.18 MHz for all hyperfine components.

Table 8. Hyperfine components and A_{ul} Einstein spontaneous emission coefficients of the (J: 1−0) transition of N_2D^+.

J'	F_1'	$F' \rightarrow J$		F_1	F	Frequency[a] (MHz)	A_{ul} (s^{-1})
1	1	0	0	1	1	77 107.4757	2.056(−5)
1	1	2	0	1	2	77 107.7671	1.542(−5)
1	1	2	0	1	1	77 107.7671	5.140(−6)
1	1	1	0	1	1	77 107.9023	5.140(−6)
1	1	1	0	1	0	77 107.9023	6.854(−6)
1	1	1	0	1	2	77 107.9023	8.568(−6)
1	2	2	0	1	1	77 109.3248	1.542(−5)
1	2	2	0	1	2	77 109.3248	5.141(−6)
1	2	3	0	1	2	77 109.6162	2.056(−5)
1	2	1	0	1	0	77 109.8104	1.142(−5)
1	2	1	0	1	2	77 109.8104	5.712(−7)
1	2	1	0	1	1	77 109.8104	8.568(−6)
1	0	1	0	1	2	77 112.1085	1.142(−5)
1	0	1	0	1	0	77 112.1085	2.285(−6)
1	0	1	0	1	1	77 112.1085	6.855(−6)

[a] The frequency uncertainty is ±2.8 kHz for all hyperfine components.

Table 9. Hyperfine components and A_{ul} Einstein spontaneous emission coefficients of the (J: 2−1) transition of N_2D^+.

J'	F_1'	$F' \rightarrow J$		F_1	F	Frequency[a] (MHz)	A_{ul} (s^{-1})
2	2	2	1	2	1	154 214.8196	7.402(−6)
2	2	2	1	2	3	154 215.0138	7.676(−6)
2	2	1	1	2	1	154 215.1417	3.701(−5)
2	2	3	1	2	3	154 215.2619	4.387(−5)
2	2	2	1	2	2	154 215.3052	3.427(−5)
2	1	1	1	0	1	154 215.3991	1.097(−4)
2	2	3	1	2	2	154 215.5533	5.483(−6)
2	1	2	1	0	1	154 215.6021	1.097(−4)
2	2	1	1	2	2	154 215.6273	1.234(−5)
2	1	0	1	0	1	154 215.8617	1.097(−4)
2	2	2	1	1	1	154 216.7277	1.110(−4)
2	3	3	1	2	3	154 216.7920	2.193(−5)
2	2	2	1	1	2	154 216.8629	3.701(−5)
2	2	1	1	1	1	154 217.0498	6.169(−5)
2	3	3	1	2	2	154 217.0834	1.755(−4)
2	3	2	1	2	1	154 217.1055	1.658(−4)
2	2	3	1	1	2	154 217.1110	1.481(−4)
2	3	4	1	2	3	154 217.1807	1.974(−4)
2	2	1	1	1	2	154 217.1850	4.113(−6)
2	3	2	1	2	3	154 217.2998	8.773(−7)
2	2	1	1	1	0	154 217.4764	8.225(−5)
2	3	2	1	2	2	154 217.5912	3.071(−5)
2	1	1	1	2	1	154 217.6972	1.371(−6)
2	1	2	1	2	1	154 217.9002	5.483(−8)
2	1	2	1	2	3	154 218.0944	4.606(−6)
2	1	0	1	2	1	154 218.1598	5.483(−6)
2	1	1	1	2	2	154 218.1828	4.113(−6)
2	1	2	1	2	2	154 218.3858	8.225(−7)
2	1	1	1	1	1	154 219.6053	2.056(−5)
2	1	1	1	1	2	154 219.7405	3.427(−5)
2	1	2	1	1	1	154 219.8083	2.056(−5)
2	1	2	1	1	2	154 219.9435	6.169(−5)
2	1	1	1	1	0	154 220.0320	2.742(−5)
2	1	0	1	1	1	154 220.0679	8.225(−5)

[a] The frequency uncertainty is ±2.1 kHz for all hyperfine components.

Database for Molecular Spectroscopy (CDMS) catalogue gives ν = 279 511.8577 MHz for the (F_1F: 4,5−3,4) strongest hyperfine component based on various works, while Crapsi et al. (2005) give 279 511.863 MHz determined from the new rotational and centrifugal distortion constants from Dore et al. (2004). These new values are respectively 26 and 31 kHz above our own determination.

4.3. N_2D^+ corrections

For all three transitions of N_2D^+, we took advantage of the similar sampling with N_2H^+ (J: 1−0) to have more comparison points. We obtained 83, 73, and 51 comparison points with a high enough signal-to-noise ratio between N_2H^+ (J: 1−0) (using Caselli et al. 1995, frequency) and N_2D^+ (J: 1−0), (J: 2−1), and (J: 3−2) transitions, respectively. The Gaussian fit to each histogram yielded

(J: 1−0): -5.1 m s^{-1} (σ = 10.5 m s^{-1})
(J: 2−1): 12.5 m s^{-1} (σ = 14.4 m s^{-1})
(J: 3−2): 18.4 m s^{-1} (σ = 8.1 m s^{-1}).

Table 10. Hyperfine components and A_{ul} Einstein spontaneous emission coefficients of the (J: 3–2) transition of N_2D^+.

J'	F_1'	$F' \rightarrow J$		F_1	F	Frequency[a] (MHz)	A_{ul} (s^{-1})
3	3	3	2	3	2	231 319.4552	6.294(−6)
3	3	3	2	3	4	231 319.5743	6.373(−6)
3	3	2	2	3	2	231 319.8904	7.049(−5)
3	3	4	2	3	4	231 319.9411	7.435(−5)
3	3	3	2	3	3	231 319.9629	6.664(−5)
3	3	4	2	3	3	231 320.3297	4.957(−6)
3	3	2	2	3	3	231 320.3981	8.812(−6)
3	2	2	2	1	2	231 321.1993	1.499(−4)
3	2	2	2	1	1	231 321.4023	4.497(−4)
3	2	1	2	1	0	231 321.4445	3.331(−4)
3	4	4	2	3	4	231 321.4756	4.461(−5)
3	3	3	2	2	3	231 321.4930	7.050(−5)
3	2	3	2	1	2	231 321.5630	5.996(−4)
3	2	1	2	1	2	231 321.7041	1.665(−5)
3	3	3	2	2	2	231 321.7411	5.640(−4)
3	3	2	2	2	1	231 321.8543	5.330(−4)
3	3	4	2	2	3	231 321.8599	6.345(−4)
3	4	4	2	3	3	231 321.8643	6.692(−4)
3	4	3	2	3	2	231 321.8645	6.555(−4)
3	2	1	2	1	1	231 321.9071	2.498(−4)
3	4	5	2	3	4	231 321.9120	7.138(−4)
3	3	2	2	2	3	231 321.9283	2.820(−6)
3	4	3	2	3	4	231 321.9836	9.104(−7)
3	2	2	2	3	2	231 321.9940	3.525(−7)
3	3	2	2	2	2	231 322.1764	9.870(−5)
3	2	3	2	3	2	231 322.3577	7.194(−9)
3	4	3	2	3	3	231 322.3722	5.736(−5)
3	2	3	2	3	4	231 322.4768	2.913(−6)
3	2	1	2	3	2	231 322.4988	3.172(−6)
3	2	2	2	3	3	231 322.5017	2.820(−6)
3	2	3	2	3	3	231 322.8654	2.518(−7)
3	2	2	2	2	1	231 323.9578	1.666(−5)
3	2	2	2	2	3	231 324.0318	1.727(−5)
3	2	2	2	2	2	231 324.2799	7.711(−5)
3	2	3	2	2	3	231 324.3955	9.870(−5)
3	2	1	2	2	1	231 324.4626	8.328(−5)
3	2	3	2	2	2	231 324.6436	1.234(−5)
3	2	1	2	2	2	231 324.7847	2.776(−5)

[a] The frequency uncertainty is ±6.2 kHz for all hyperfine components.

Table 11. Hyperfine components and A_{ul} Einstein spontaneous emission coefficients of the (J: 4–3) transition of N_2D^+.

J'	F_1'	$F' \rightarrow J$		F_1	F	Frequency[a] (MHz)	A_{ul} (s^{-1})
4	4	4	3	4	3	308 419.723	5.330(−6)
4	4	4	3	4	5	308 419.794	5.361(−6)
4	4	3	3	4	3	308 420.188	1.028(−4)
4	4	5	3	4	5	308 420.218	1.053(−4)
4	4	4	3	4	4	308 420.231	9.896(−5)
4	4	5	3	4	4	308 420.655	4.386(−6)
4	4	3	3	4	4	308 420.696	6.853(−6)
4	3	3	3	2	3	308 421.627	1.790(−4)
4	5	5	3	4	5	308 421.764	7.018(−5)
4	4	4	3	3	4	308 421.765	1.028(−4)
4	3	3	3	2	2	308 421.991	1.432(−3)
4	3	2	3	2	1	308 421.993	1.353(−3)
4	3	4	3	2	3	308 422.056	1.611(−3)
4	3	3	3	4	3	308 422.120	1.399(−7)
4	4	4	3	3	3	308 422.132	1.542(−3)
4	3	2	3	2	3	308 422.134	7.161(−6)
4	4	3	3	3	2	308 422.162	1.511(−3)
4	4	5	3	3	4	308 422.189	1.645(−3)
4	5	4	3	4	3	308 422.195	1.668(−3)
4	5	5	3	4	4	308 422.200	1.684(−3)
4	5	6	3	4	5	308 422.230	1.754(−3)
4	4	3	3	3	4	308 422.231	2.098(−6)
4	5	4	3	4	5	308 422.266	8.664(−7)
4	3	2	3	2	2	308 422.498	2.506(−4)
4	3	4	3	4	3	308 422.549	1.727(−9)
4	4	3	3	3	3	308 422.598	1.322(−4)
4	3	4	3	4	5	308 422.621	2.127(−6)
4	3	2	3	4	3	308 422.628	2.238(−6)
4	3	3	3	4	4	308 422.628	2.098(−6)
4	5	4	3	4	4	308 422.703	8.577(−5)
4	3	4	3	4	4	308 423.057	1.088(−7)
4	3	3	3	3	2	308 424.094	1.119(−5)
4	3	3	3	3	4	308 424.163	1.133(−5)
4	3	3	3	3	3	308 424.530	1.185(−4)
4	3	4	3	3	4	308 424.592	1.322(−4)
4	3	2	3	3	2	308 424.602	1.253(−4)
4	3	4	3	3	3	308 424.959	8.812(−6)
4	3	2	3	3	3	308 425.037	1.567(−5)

[a] The frequency uncertainty is ±25 kHz for all hyperfine components.

The corresponding correction with respect to NH_3(1, 1) is

(J: 1–0): 35.7 m s^{-1} or − 9.2 (±2.7) kHz
(J: 2–1): 53.3 m s^{-1} or − 27 (±7.4) kHz
(J: 3–2): 59.2 m s^{-1} or − 49 (±6.7) kHz.

Direct comparison of the reference position with NH_3(1, 1) spectrum yields

(J: 1–0): 37.7 m s^{-1} (σ = 0.85 m s^{-1})
(J: 2–1): 47.7 m s^{-1} (σ = 0.92 m s^{-1})
(J: 3–2): 63.6 m s^{-1} (σ = 4.7 m s^{-1}).

4.4. Rotational constants and Einstein-A coefficients

Except for the N_2H^+ (J: 3–2) line, which has only one measurement, we used the averaged comparisons for correcting the frequencies of all these transitions.

From these new frequencies, we derived the rotation (B) and centrifugal distortion (D) constants for N_2H^+ and N_2D^+, using the hyperfine constants given by Caselli et al. (1995) and Dore et al. (2004), respectively. The error budget was estimated by adding 1σ to one of the frequency measurements and subtracting 1σ to the other, which we used to determine B and D, e.g. +2.7 kHz to the N_2D^+ (J: 1–0) line and −6.7 kHz for the N_2D^+ (J: 3–2) line. For the N_2H^+ (J: 3–2) transition, as we have only one measurement, we took the average of the 1σ dispersion for all the other transition measurements as a probable dispersion for that measurement if we had had as many observations. We found an average velocity dispersion of 11.5 m s^{-1}, which corresponds to 10.7 kHz at that frequency. The new constants are listed in Table 1. As expected from Amano et al. (2005) making use of the Caselli et al. (1995) frequency determination of N_2H^+ and the related Dore et al. (2004) N_2D^+ measurements, their rotational constants are different from ours by an amount directly related to the difference between C_3H_2 and NH_3 velocity

Table 12. Hyperfine components and A_{ul} Einstein spontaneous emission coefficients of the (J: 5–4) transition of N_2D^+.

J'	F'_1	$F' \rightarrow J$		F_1	F	Frequency[a] (MHz)	A_{ul} (s^{-1})
5	5	5	4	5	4	385 514.088	4.587(−6)
5	5	5	4	5	6	385 514.125	4.601(−6)
5	5	4	4	5	4	385 514.562	1.346(−4)
5	5	6	4	5	6	385 514.584	1.363(−4)
5	5	5	4	5	5	385 514.591	1.310(−4)
5	5	6	4	5	5	385 515.050	3.894(−6)
5	5	4	4	5	5	385 515.065	5.607(−6)
5	4	4	4	3	4	385 516.051	2.082(−4)
5	5	5	4	4	5	385 516.136	1.346(−4)
5	6	6	4	5	6	385 516.141	9.734(−5)
5	4	4	4	5	4	385 516.406	6.922(−8)
5	4	3	4	3	2	385 516.474	3.059(−3)
5	4	4	4	3	3	385 516.480	3.123(−3)
5	4	5	4	3	4	385 516.516	3.331(−3)
5	4	3	4	3	4	385 516.553	4.249(−6)
5	5	5	4	4	4	385 516.560	3.230(−3)
5	5	4	4	4	3	385 516.568	3.198(−3)
5	5	6	4	4	5	385 516.595	3.364(−3)
5	6	5	4	5	4	385 516.599	3.388(−3)
5	6	6	4	5	5	385 516.607	3.407(−3)
5	5	4	4	4	5	385 516.610	1.661(−6)
5	6	7	4	5	6	385 516.627	3.504(−3)
5	6	5	4	5	6	385 516.636	8.045(−7)
5	4	5	4	5	4	385 516.871	5.721e−10
5	4	3	4	5	4	385 516.907	1.731(−6)
5	4	5	4	5	6	385 516.908	1.673(−6)
5	4	4	4	5	5	385 516.908	1.661(−6)
5	4	3	4	3	3	385 516.982	2.677(−4)
5	5	4	4	4	4	385 517.034	1.645(−4)
5	6	5	4	5	5	385 517.102	1.150(−4)
5	4	5	4	5	5	385 517.373	5.663(−8)
5	4	4	4	4	3	385 518.412	8.328(−6)
5	4	4	4	4	5	385 518.454	8.376(−6)
5	4	4	4	4	4	385 518.878	1.546(−4)
5	4	3	4	4	3	385 518.914	1.606(−4)
5	4	5	4	4	5	385 518.919	1.645(−4)
5	4	5	4	4	4	385 519.343	6.853(−6)
5	4	3	4	4	4	385 519.379	1.071(−5)

[a] The frequency uncertainty is ±58 kHz for all hyperfine components.

Table 13. Hyperfine components and A_{ul} Einstein spontaneous emission coefficients of the (J: 6–5) transition of N_2D^+.

J'	F'_1	$F' \rightarrow J$		F_1	F	Frequency[a] (MHz)	A_{ul} (s^{-1})
6	6	6	5	6	5	462 601.05	4.014(−6)
6	6	6	5	6	7	462 601.06	4.021(−6)
6	6	5	5	6	5	462 601.53	1.660(−4)
6	6	7	5	6	7	462 601.54	1.673(−4)
6	6	6	5	6	6	462 601.55	1.627(−4)
6	6	5	5	6	6	462 602.02	4.744(−6)
6	6	7	5	6	6	462 602.03	3.485(−6)
6	5	5	5	4	5	462 603.04	2.378(−4)
6	6	6	5	5	6	462 603.10	1.660(−4)
6	7	7	5	6	7	462 603.11	1.255(−4)
6	5	5	5	6	5	462 603.32	3.920(−8)
6	5	4	5	4	3	462 603.50	5.651(−3)
6	5	5	5	4	4	462 603.51	5.707(−3)
6	5	6	5	4	5	462 603.53	5.945(−3)
6	5	4	5	4	5	462 603.54	2.936(−6)
6	6	5	5	5	4	462 603.56	5.780(−3)
6	6	6	5	5	5	462 603.56	5.811(−3)
6	6	5	5	5	6	462 603.58	1.372(−6)
6	6	7	5	5	6	462 603.59	5.977(−3)
6	7	6	5	6	5	462 603.59	6.002(−3)
6	7	7	5	6	6	462 603.60	6.022(−3)
6	7	6	5	6	7	462 603.60	7.424(−7)
6	7	8	5	6	7	462 603.61	6.148(−3)
6	5	6	5	6	5	462 603.81	2.320e − 10
6	5	4	5	6	5	462 603.81	1.411(−6)
6	5	5	5	6	6	462 603.81	1.372(−6)
6	5	6	5	6	7	462 603.81	1.378(−6)
6	5	4	5	4	4	462 604.00	2.906(−4)
6	6	5	5	5	5	462 604.04	1.962(−4)
6	7	6	5	6	6	462 604.09	1.448(−4)
6	5	6	5	6	6	462 604.30	3.317(−8)
6	5	5	5	5	4	462 605.35	6.605(−6)
6	5	5	5	5	6	462 605.37	6.626(−6)
6	5	5	5	5	5	462 605.83	1.886(−4)
6	5	4	5	5	4	462 605.85	1.938(−4)
6	5	6	5	5	6	462 605.86	1.962(−4)
6	5	6	5	5	5	462 606.32	5.606(−6)
6	5	4	5	5	5	462 606.32	8.073(−6)

[a] The frequency uncertainty is ±0.11 MHz for all hyperfine components.

determinations. The difference (5.3 kHz for $B(N_2H^+)$ and 9.2 kHz for $B(N_2D^+)$) is significantly greater than the error estimate (conservatively given to be 2.5 and 1.7 kHz for us and 1.3 and 1.2 kHz for Amano et al. 2005). It would be interesting to repeat the Amano et al. (2005) analysis with our new frequency determinations to secure these values better.

Line strengths, from which Einstein-A coefficients are defined, are determined from the reduced transition matrix elements of the dipole moment operator:

$$S(1 \rightarrow 2) = |\left\langle \psi_1 || \hat{d} || \psi_2 \right\rangle|^2 \quad (1)$$

where $|\psi_1>$ and $|\psi_2>$ are the wave-functions of the two levels involved in the radiative transition. In the case of hyperfine structures, the wave-functions can be defined according to an expansion on Hund's case (b) wave-functions, the coefficients being determined by diagonalization of the hyperfine Hamiltonian. In the case of N_2H^+ and N_2D^+, the mixing of states is low so that a given hyperfine wave-function can be accurately defined as a pure Hund's case (b) wave-function. Doing so, the line strengths can be expressed in a closed form (Gordy & Cook 1984) and, for N_2H^+, the relevant expressions being given in Daniel et al. (2006). The Einstein-A coefficients are then given by

$$A_{JF_1F \rightarrow J'F'_1F'} = \frac{64\pi^4}{3hc^3} \mu^2 \nu^3_{JF_1F \rightarrow J'F'_1F'} \times \frac{J}{[F]} s_{JF_1F \rightarrow J'F'_1F'}. \quad (2)$$

(This is the same equation as in Daniel et al. 2006, but corrected for two typographical errors).

The calculated line frequencies and A_{ul} coefficients (the dipole moment – μ = 3.37 D – is taken from Botschwina 1984) are given in Tables 2 to 10 for all rotational transitions from (J: 1–0) to (J: 6–5) for both N_2H^+ and N_2D^+. The frequency uncertainty is estimated by varying the rotational B and D constants by $\pm 1\sigma$.

5. Conclusions

New, more accurate rotational constants and line frequencies are given along with the detailed Einstein spontaneous coefficients (A_{ul}) for each of the hyperfine components. The main prestellar core LSR velocity is 2.3670 (±0.0004) km s^{-1}.

Acknowledgements. We thank an anonymous referee for her/his critical reading that helped to improve the manuscript.

References

Amano, T., Hirao, T., & Takano, J. 2005, J. Mol. Spectro., 234, 170
Botschwina, P. 1984, Chem. Phys. Lett., 107, 535
Caselli, P., Myers, P. C., & Thaddeus, P. 1995, ApJ, 455, L77
Crapsi, A., Caselli, P., Walmsley, C. M., et al. 2005, ApJ, 619, 379
Daniel, F., Cernicharo, J., & Dubernet, M.-L. 2006, ApJ, 648, 461
Dore, L., Caselli, P., Beninati, S., et al. 2004, A&A, 413, 1177
Gerin, M., Pearson, J. C., Roueff, E., Falgarone, E., & Phillips, T. G. 2001, ApJ, 551, L193
Gordy, W., & Cook, R. L. 1984, Microwave molecular spectra Techniques of chemistry, 18
Hougen, J. T. 1972, J. Chem. Phys., 57, 4207
Kuiper, T. B. H., Langer, W. D., & Velusamy, T. 1996, ApJ, 468, 761
Kukolich, S. G. 1967, Phys. Rev., 156, 83
Lee, C. W., Myers, P. C., & Tafalla, M. 1999, ApJ, 526, 788
Pagani, L., Gallego, A. T., & Apponi, A. J. 2001, A&A, 380, 384
Pagani, L., Gallego, A. T., & Apponi, A. J. 2002, A&A, 381, 1094 (Erratum)
Pagani, L., Bacmann, A., Motte, F., et al. 2004, A&A, 417, 605
Pagani, L., Pardo, J.-R., Apponi, A. J., Bacmann, A., & Cabrit, S. 2005, A&A, 429, 181
Pagani, L., Bacmann, A., Cabrit, S., & Vastel, C. 2007, A&A, 467, 179
Roberts, H., & Millar, T. J. 2007, A&A, 471, 849
Schmid-Burgk, J., Muders, D., Müller, H. S. P., & Brupbacher-Gatehouse, B. 2004, A&A, 419, 949
Swade, D. A. 1989, ApJS, 71, 219
Tafalla, M., Myers, P. C., Caselli, P., Walmsley, C. M., & Comito, C. 2002, ApJ, 569, 815
Tafalla, M., Myers, P. C., Caselli, P., & Walmsley, C. M. 2004, A&A, 416, 191
Willacy, K., Langer, W. D., & Velusamy, T. 1998, ApJ, 507, L171